

# Dynamic characterization of shallow foundations with full-scale tests

Aldo Madaschi<sup>1</sup>, Alessandro Gajo<sup>1</sup>, Marco Molinari<sup>1</sup>, Daniele Zonta<sup>1</sup>

<sup>1</sup>*Department of Civil, Environmental and Mechanical Engineering - University of Trento, via Mesiano, 77 38123 Trento, aldo.madaschi@unitn.it*

**Abstract** – This work provides a detailed description of the full-scale experimental tests performed on the dynamic behavior of a shallow foundation under intermediate strains. A wind tower supported by the foundation was submitted to a snap-off test inducing free oscillations of non-negligible amplitude in the whole system. The motion induced was measured with a digital camera, seismometers and accelerometers attached to the surrounding ground surface and to the wind tower. An innovative interpretation technique based on optimizing a few meaningful parameters obtained from the recorded time histories was necessitated by the heterogeneity of the data collected and the accuracy needed to deduce the behavior of the foundation plinth. The analyses showed that the rotational stiffness of the foundation plinth was roughly 10 times greater than that of the base joint, which in turn was about 1 order of magnitude greater than that of the wind tower.

## I. INTRODUCTION

The dynamic response of shallow foundations is of great interest in a number of civil engineering problems ranging from the design of foundations for vibrating apparatuses ([1], [2]) to the dynamic response of structures under seismic action ([3], [4]).

From a theoretical standpoint, most of the analyses in the literature are based on the assumption of an elastic soil response. From an experimental standpoint, most of the analyses in the literature concern physical models and centrifuge tests ([5], [6], [7]), such as the model tests performed by [8] on offshore wind towers. To the best of the authors' knowledge, very few experimental analyses have been published on small-scale, shallow footings resting on natural soils (see [9] and [10]), and none at all on large-scale, real shallow footings.

This work describes a full-scale experimental analysis on the dynamic behavior of a wind tower's shallow foundation, consisting of a square plinth, 0.90 m thick and 4.50 m wide, resting on a coarse granular soil lying over a thick layer of silt. Dynamic excitation was induced by means of a snap-off test (SOT): the wind tower was pulled with a cable anchored to a truck, then the pulling force was suddenly released, thus producing a wide-amplitude free vibration of the tower. During the free oscillations of the

wind tower, the displacements were accurately monitored, as were the accelerations of the tower and foundation, and the velocity of the ground surface surrounding the foundation plinth. The heterogeneity of the data collected and the accuracy needed to deduce the behavior of the foundation plinth made it necessary to develop a specific, innovative interpretation method to identify the engineering parameters describing the foundation's dynamic response (further details can be found in [11]).

## II. WIND TOWER AND SUBSOIL

The structure investigated is an 11 kW downwind generator manufactured by Gaia-Wind and installed at the Trento Research Wind Farm located in the industrial area of Gardolo, near the town of Trento. The wind turbine is 13 m in diameter and has a pair of blades designed to rotate at a predetermined constant frequency of about 2 Hz under operational conditions. The overall mass of the wind turbine is 943 kg; and the tower supporting the nacelle is 18.15 m high (see the setup shown in Figure 1) high and consists of tapered hollow S355 steel pipe 6 mm thick, with a circular cross-section with an external diameter tapered linearly from 938 mm at the base to 410 mm at the top. The base flange is anchored by means of 16 bolts 36 mm in diameter to a square concrete foundation plinth with 4.5 m side and 0.9 m thickness. During the installation, the steel tower was plumbed with the base flange resting above a series of nuts threaded onto the anchor bolts 100 mm above the upper surface of the plinth. Once plumbed, the base flange was tightened to the anchors with a second series of upper bolts, while the gap between the base flange and the concrete plinth was filled with expansive mortar to ensure an even contact.

Modal extraction from SHT signals enabled the identification of 7 vibration modes in the frequency range from 1.3 Hz to 25 Hz [12]. As expected, the first two bending modes - the first in a N-S and the second in an E-W direction - are strongly coupled, with modal frequencies of 1.345 Hz and 1.356 Hz, respectively.

The joint stiffness was evaluated using accurate nonlinear FEM simulations. The results of the FEM simulations showed that the response of the base joint was fairly nonlinear, ranging between  $7 \times 10^8$  N m/rad and  $10 \times 10^8$  N m/rad for the bending moments transmitted during the

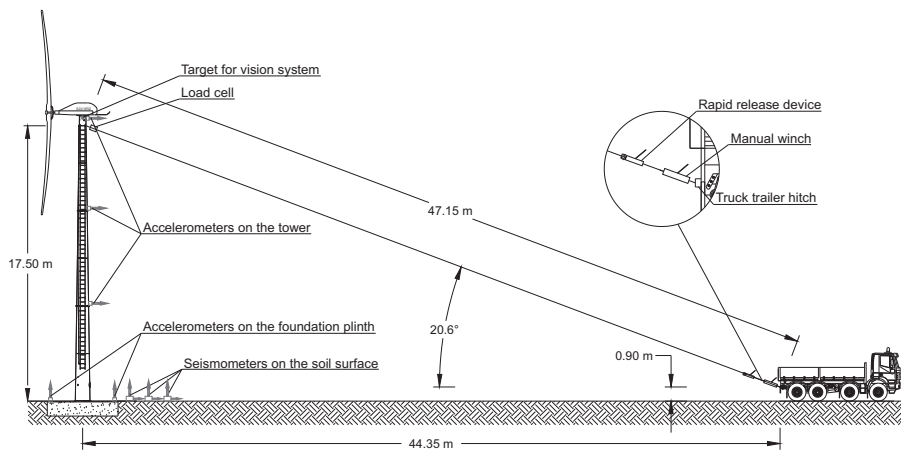


Figure 1. Setup of the snap-off test.

### SOT.

The subsoil in the wind field is mainly alluvial and consists of silt and gravel layers. After the site had been destined for industrial purposes, the upper soil layer was removed and a large embankment was built with very stiff compacted coarse till. The resulting embankment thickness is 4.00 m, under which there is a layer of silt 3.50 m thick, a layer of coarse sand 1.50 m thick, and gravel down to depths in excess of 15.00 m. The foundation plinth rests on the compacted coarse till, which is about 23.00 m thick underneath the plinth. The ground water table is 2.00-4.00 m deep and is strongly affected by the hydrometric level of the Adige river (flowing about 1 km away from the site).

Soil stiffness was assessed with seismic tests using multichannel analysis of surface waves (MASW) performed by the Trento Province Geological Survey Service. Two tests were performed and the results are given in Figure 2.

### III. TEST SETUP

The experimental setup used for the SOT is shown in Figure 1: the wind tower was first pulled with a cable anchored to a truck using a manual winch, then the pulling force was suddenly released leading to wide-amplitude, free vibrations in the wind tower. The maximum pulling force ( $\simeq 5$  kN) was about 1/4 of the theoretically allowable static horizontal force.

The following instruments were installed for the SOT:

- 4 horizontal uni-directional accelerometers (PCB 393C, max range 2.5 g, sensitivity 1000 mV/g) installed at elevations of 6.05 m, 12.10 m, and 18.15 m; three of them measured along the pulling direction and one transversely;
- 3 vertical uni-directional accelerometers (PCB 393B12, max range 0.5 g, sensitivity 9630 mV/g,) mounted on the upper face of the foundation plinth;
- 4 tri-directional seismometers (Solgeo GET.3D, sensitivity 12.5 mm/sec) mounted on the asphalted surface of the ground at increasing distances from the northern edge of the plinth;
- 1 load cell (max range 20 kN, accuracy 0.8%) for measuring the pulling force;
- 1 fast-shooting digital camera (MotionBlitz Cube 2, resolution 1280x1024 pixel) for recording lateral displacements of an optical target installed on the top of the wind tower, during the free oscillations.

Data were acquired at a sampling frequency of 1250 Hz for the accelerometers and 125 Hz for the seismometers, while the digital camera took 125 frames per second. The history of the free oscillations of the top of the wind tower was reconstructed by post-processing the images obtained with the digital camera with an approximate of about 1.0 mm in the horizontal target positions.

Five SOTs were performed with different pulling forces ranging between 1.7 and 5 kN (more precisely: 1.78, 3.37, 4.76, 4.71 and 3.37 kN for test no. 1 to 5, respectively). The maximum pulling force applied during the SOTs corresponds to a safety factor of  $F_s = 56/4.7 = 11.9$  for the foundation's failure. Concerning the soil pressure distribution under the plinth, if a linear distribution is assumed during the SOT, then the soil pressure is expected to range between 18 and 27 kPa.

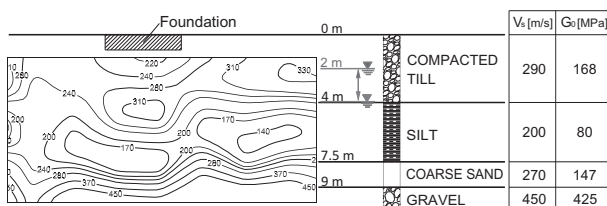


Figure 2. Results of MASW seismic tests and stratigraphy.

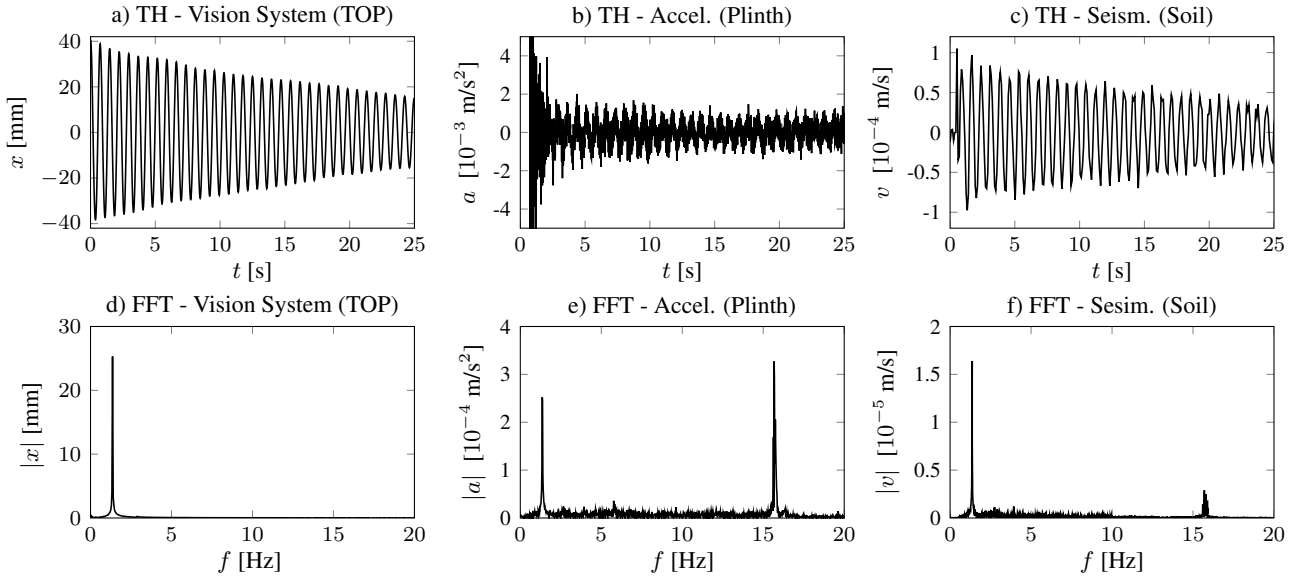


Figure 3. Time histories and FFT analyses for the SOT 3: (a and d) horizontal displacement at the top of the tower; (b and e) vertical acceleration at the foundation plinth; (c and f) vertical velocity at the soil surface

#### IV. RESULTS OF SNAP-OFF TESTS

This Section describes the measurements recorded during the free oscillations of the wind tower, for the sake of brevity, we focus here on the data collected in test No. 3 ( $F_{\text{pull}} = 4.76$  kN). Figure 3 shows the time histories (TH) and the Fast Fourier Transforms (FFT) of three different physical quantities measured during the free oscillation phase.

The history of horizontal displacement of the top of the wind tower (Fig. 3a) shows an harmonic motion at around the first natural frequency (approximately 1.3 Hz). The regularity of the harmonic oscillations involving the first oscillation mode can easily be appreciated. The initial amplitude of oscillation was nearly 40 mm that was only slightly damped.

The acceleration history of the top of the wind tower (Fig. 3b) shows that, after the initial perturbation induced by the sudden release of the pulling force, the time history consists of 2 harmonic signals having frequencies of about 1.3 Hz and 16 Hz (Figure 4e). The former signal (1.3 Hz) is clearly related to the first vibration mode. The 16 Hz signal is observable only in tests Nos. 3 and 4, and it might relate to an external excitation source.

#### V. ANALYSIS OF EXPERIMENTAL RESULTS

The main point of interest is whether the response is nonlinear and, if so, what causes this nonlinearity. We have already seen that the free motion is clearly dominated by an individual frequency, which is apparently near 1.3 Hz. The basic assumption here was therefore that the time-domain

response of the tower could be interpreted as that of a nonlinear oscillator with a single degree of freedom and with frequency and damping that vary with oscillation amplitude.

The time-domain analysis included the following steps. First a kinematic analysis of the response recorded at the top of the tower was conducted to identify the relationship describing how frequency and damping rate depended on oscillation amplitude. Then a parametric nonlinear equivalent mechanical model of the structure-soil system was defined. The amplitude-dependent base stiffness that best fitted the observed response was identified.

The displacements measured on the images obtained with the digital camera ( $x$  in Fig. 3a) were first analyzed to assess how frequency changed with vibration amplitude. For this purpose, small time windows of the displacements measured at the top of the tower were directly fitted using the following theoretical harmonic motion:

$$x(t) = x_0 \sin(\omega t + \phi) \quad (1)$$

and keeping angular frequency  $\omega$ , amplitude  $x_0$  and phase shift  $\phi$ , as free parameters. The fitting procedure was repeated, shifting the time windows in intervals of 1/10th of the natural period of the tower. The fitting was done in the time domain using a minimization algorithm implemented in the commercial code Mathematica (Wolfram Research, 2012).

After identifying the natural frequency, the structural damping  $\xi$  was assessed in a second step, by fitting the displacements measured within the small time windows with

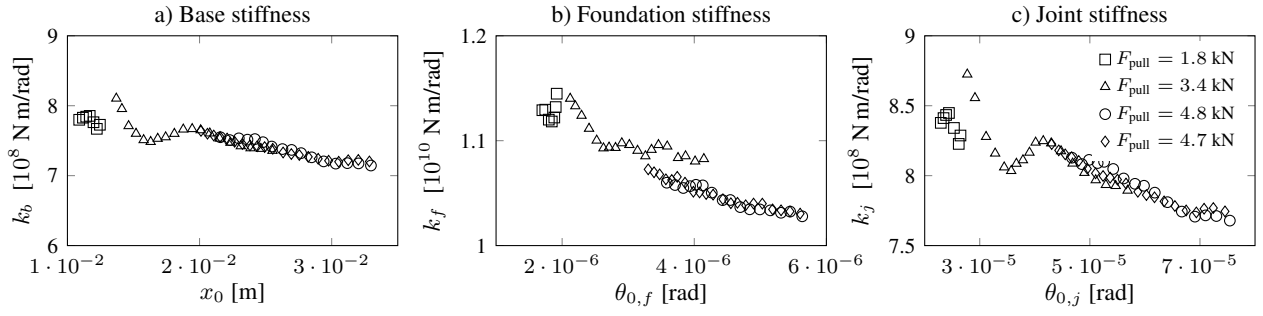


Figure 4. Stiffness evolutions during SOT from model fitting: (a) global base rotational; (b) foundation; (c) base joint.

the following equation:

$$\tilde{x}(t) = \tilde{x}_0 \sin(\omega t + \phi) \exp(-\xi \omega t) \quad (2)$$

where  $\tilde{x}_0$  and  $\xi$  are two unknown parameters, while  $\omega$  and  $\phi$  are those ascertained from the previous fitting step. This two step procedure allows to increase the accuracy of the frequency estimation with respect to the simultaneous optimization of the four unknown parameters.

Since the tower's motion involves only one vibration mode, it is reasonable to approximate the wind tower to a single DOF oscillator characterized by a global modal stiffness  $k$ , and a global modal mass  $m$ , as shown in Figure 5. The global modal stiffness  $k$  is assumed to consist of two fractions, i.e. the total rotational modal stiffness at the base,  $k_b$  (resulting from the rotational modal stiffnesses of both the base joint and the foundation plinth,  $k_j$  and  $k_f$ , both expressed in Nm/rad), and the translational tower modal stiffness,  $k_t$  (expressed in N/m). The global modal stiffness,  $k = \bar{k}(k_b)$  can thus be deduced with ease from the expression of the stiffness of two springs in series, namely:

$$k = \bar{k}(k_b) = \left( \frac{1}{k_t} + \frac{1}{k_b/h^2} \right)^{-1} \quad (3)$$

where  $h$  is the tower height. The nonlinear effects are assumed to be concentrated either in the foundation (in  $k_f$ )

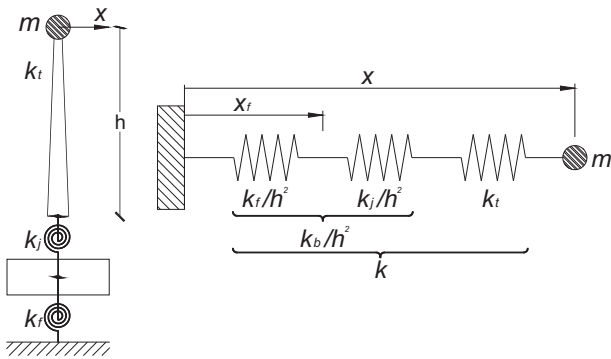


Figure 5. Analytical model for identification procedure.

or in the base joint (in  $k_b$ ), whereas a linear behavior is assumed for the tower (in  $k_t$ ). Given the assumed nonlinear effects, the global modal stiffness,  $k$ , and modal mass,  $m$ , generally depend on the base rotational stiffness  $k_b$ , namely  $k = \bar{k}(k_b)$  and  $m = \bar{m}(k_b)$ , and are related to each other through the modal frequency according to the formula:

$$\bar{k}(k_b) = \omega^2 \bar{m}(k_b). \quad (4)$$

The tower stiffness  $k_t$  in Eq. (3) was estimated numerically using an accurate linear elastic FEM model and it was assumed to be equal to  $k_t = 104075$  kN/m.

The global modal mass  $m = \bar{m}(k_b)$  was obtained in a similar way, using the same refined modal 3D FEM analysis in which a rotational spring  $k_b$  was assumed at the tower base joint and resulted:

$$\bar{m}(k_b) = 1352.02 + \frac{1.27536 \times 10^7}{k_b}. \quad (5)$$

Taking into account the modal frequency estimates through the minimization procedure, and introducing Eqs. (5) and (4) in Eq. (3), a nonlinear equation in terms of  $k_b$  was obtained, which was easily solved by obtaining the results shown in Fig. 4a.

The experimental assessments in Figure 4a clearly show that the base stiffness depends on the oscillation amplitude,  $x_0$ , at the top of the tower, i.e.  $\bar{k}_b(x_0)$ . Due to the dependence of  $k = \bar{k}(k_b)$  and  $m = \bar{m}(k_b)$ , even the modal stiffness  $k$  and modal mass  $m$ , can be considered in turn as functions of the oscillation amplitude,  $x_0$ , namely  $k = \bar{k}(x_0)$  and  $m = \bar{m}(x_0)$ . Applying the standard concepts of structural dynamics and considering the modal acceleration amplitudes ( $\ddot{z}_{1,0f}$  and  $\ddot{z}_{3,0f}$ ) measured on the foundation plinth by accelerometers A1 and A3, we can calculate the foundation's stiffness, which amounts to

$$k_f = \bar{k}_f(x_0) = \frac{\omega^2}{\ddot{z}_{1,0f} + \ddot{z}_{3,0f}} \frac{d}{h} \bar{k}(x_0) x_0 \quad (6)$$

where is the horizontal distance between the accelerometers mounted on the foundation plinth. The base joint stiffness can easily be deduced by substituting Eq. (6) in the

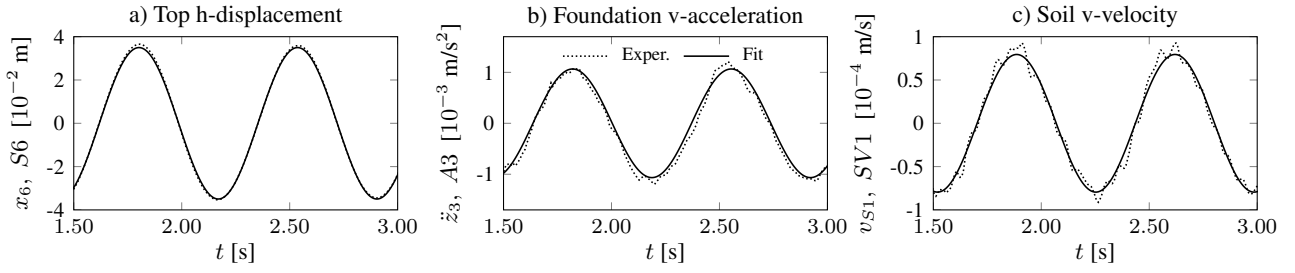


Figure 6. Comparisons between acquisition and analytical signals (Test 3): (a) horizontal displacement of the top ( $S6$ ); (b) vertical acceleration on the foundation plinth ( $A3$ ); (c) vertical velocity at 0.75 m far from the edge of plinth ( $SV1$ )

expression of the stiffness of in-series springs

$$k_j = \bar{k}_j(x_0) = \left( \frac{1}{\bar{k}_b(x_0)} - \frac{1}{\bar{k}_f(x_0)} \right)^{-1} \quad (7)$$

The modal amplitudes of the base joint rotation,  $\theta_{0j}$ , and foundation rocking,  $\theta_{0f}$ , amount to

$$\theta_{0j} = \frac{k}{k_j} h x_0 \quad \text{and} \quad \theta_{0f} = \frac{\ddot{z}_{1,0f} + \ddot{z}_{3,0f}}{\omega^2} \frac{1}{d} \quad (8)$$

The base joint and foundation modal stiffnesses,  $k_j$  and  $k_k$ , obtained with Eqs. (7-6), are plotted in terms of base joint and foundation rotations, respectively,  $\theta_{0j}$  and  $\theta_{0f}$ , in Figure 4b and 4c. The foundation's stiffness is clearly about 10 times greater than that of the base joint. The foundation's rotational stiffness decreases slightly with increasing rotation amplitudes. Finally the rotational stiffnesses depend only on the rotation amplitude and are fairly independent of the initial pulling force.

## VI. VALIDATION AND DISCUSSION

Figure 6 shows the comparison between measurements and optimized, theoretical results concerning the displacements at the tower top, the vertical acceleration on the foundation plinth and finally the vertical velocity 1.0 m far from the foundation plinth.

For the sake of completeness, Figure 7a and Figure 7b show the response in terms of bending moment at the base,  $M_b$ , versus the amplitude rotation of the base joint and foundation plinth, respectively. From Figure 7, it is easy to see that both the foundation and the base joint responses are slightly nonlinear.

It is worth adding that, from the analytical solution obtained with BEM by Capuani et al. [13], and for the present geometry and frequency content (1.3 Hz), a quasi-static foundation rocking occurs with a negligible geometric dissipation and no phase change between harmonic excitation and foundation response. As a result, any foundation damping can be expected to be induced by soil dissipation alone (due to its constitutive behavior), not by geometric dissipation.

## VII. ANALYSIS OF GEOMETRIC ATTENUATION AROUND THE PLINTH

The geometric attenuation of the vertical oscillations on the surface of the ground around the foundation plinth was assessed by analyzing the vertical velocities measured by the seismometers. The vertical displacement of the edge of the foundation plinth is given by  $\theta_{0f} B/2$ , while for the surface of the ground at each seismometer it is obtained from the measured vertical velocity amplitudes,  $v_{Si,0}/\omega$  (at seismometer), through, so we can define the geometric attenuation coefficients  $\delta_{Si}$  with respect to the displacement of the foundation's edge, according to the formula

$$\delta_{Si} = \frac{v_{Si,0}}{\omega \theta_{0f} B/2}. \quad (9)$$

The spatial variations in the geometric attenuations are shown in Figure 8, for two values of foundation bending moment (50 and 18 kN m), so the curves in Figure 8 represent the deformed shapes of the ground's surface near the foundation plinth, scaled in relation to the vertical displacements of the foundation's edge.

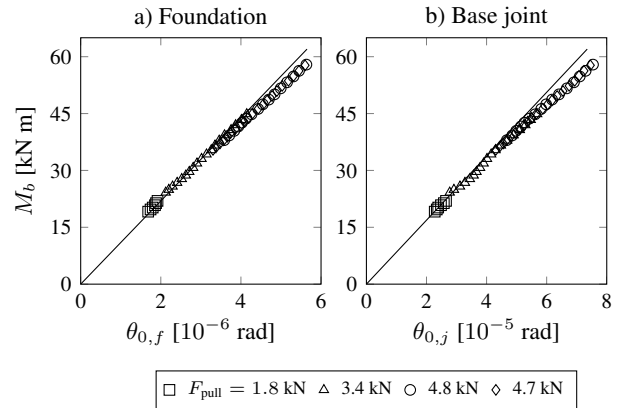


Figure 7. Bending moment-rotation curves.

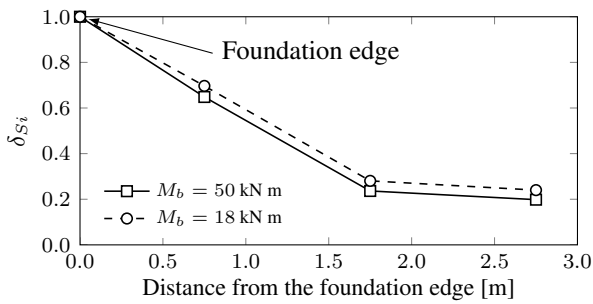


Figure 8. Geometric attenuation coefficient versus the distance from the edge of the plinth.

### VIII. CONCLUSIONS

This work provides a detailed description of a full-scale experimental analysis performed on the dynamic behavior of a shallow footing at intermediate strains. The foundation supports a wind tower was subjected to a series Snap-Off Tests. The motion induced was measured with a digital camera, seismometers and accelerometers applied to the surrounding ground and the wind tower.

A specific, innovative interpretation technique based on a procedure for optimizing a few meaningful parameters of the recorded time histories was used. The technique relied on a time-domain analysis that enabled the dependence of frequency and damping ratio on the oscillation amplitude to be analyzed within short time windows (see [11]).

Table 1. Comparison between the base stiffness estimates

Method	$k_b$ $\left[10^8 \frac{\text{N m}}{\text{rad}}\right]$	$k_j$ $\left[10^8 \frac{\text{N m}}{\text{rad}}\right]$	$k_f$ $\left[10^8 \frac{\text{N m}}{\text{rad}}\right]$
Ela. Th. ( $E = 180$ MPa, $\nu = 0.2$ )	-	-	92
FEM base joint	-	$7 \div 10$	-
SOT (fitting)	$7.2 \div 8$	$7.7 \div 8.5$	$100 \div 115$
SOT (static pull)	$4.3 \div 13$	-	-

The resulting rotational stiffnesses are compared with static measurements and conventional stiffness assessments in Table 1. The analyses show that the rotational stiffness of the foundation plinth was roughly ten times greater than that of the base joint, which in turn was about one order of magnitude greater than the stiffness of the wind tower. The rotational stiffness of the foundation plinth had negligible effects on the tower's response (in our experimental setup), and tower oscillation and foundation rocking were decoupled from one another.

The seismometer measurements performed on the surface of the ground surrounding the foundation plinth enabled the assessment of the geometric attenuation of the surface vibrations induced by foundation rocking. Due to

the quasi-static foundation rocking, the geometric attenuation deduced from our seismometer measurements also gives us a measure of the quasi-static deformations of the ground surface around the rocking foundation. To the best of the authors' knowledge, no such findings have been published elsewhere in the literature.

### IX. REFERENCES

- [1] G.C. Gazetas, "Analysis of machine foundation vibrations: state of the art", International J. of Soil Dyn. and Earthq. Eng., 2(1):2-42, 1983.
- [2] Y. Nii, "Experimental Half-Space Dynamic Stiffness", J. of Geotech. Eng., 113(11):1359-1373, 1988.
- [3] J.P. Wolf, "Dynamic Soil-Structure Interaction. Englewood Cliffs" PTR Prentice Hall, 1994.
- [4] H.B. Seed, "Soil-structure interaction analysis for seismic response" ASCE, 101(5):439-457, 1975.
- [5] G.C. Gazetas, K.H. Stokoe, "Free Vibration of Embedded Foundations: Theory versus Experiment", J. Geotech. Eng., 117(9):1382-1401, 1991.
- [6] M. Maugeri, G. Musumeci, D. Novità, C.A. Taylor, "Shaking table test of failure of a shallow foundation subjected to an eccentric load", Soil Dyn. Earthq. Eng., 20:435-444, 2000.
- [7] S. Gajan, B.L. Kutter, et al., "Centrifuge modeling of load-deformation behavior of rocking shallow foundations", Soil Dyn. Earthq. Eng., 25(7-10):773-783, 2005.
- [8] S. Bhattacharya, S. Adhikari, "Experimental validation of soil-structure interaction of offshore wind turbines", Soil Dyn. Earthq. Eng., 31(5-6):805-816, 2011.
- [9] C.B. Crouse, G. Liang, G. Martin, "Experimental foundation impedance functions", J. Geotech. Eng. - ASCE, 111(6):819-822, 1985.
- [10] C.B. Crouse, B. Hushmand, J.E. Luco, et al., "Foundation Impedance Function - Theory versus Experiment", J. Geotech. Eng. - ASCE, 116(3):432-449, 1990.
- [11] A. Madaschi, A. Gajo, M. Molinari, and D. Zonta, "Characterization of the Dynamic Behavior of Shallow Foundations with Full-Scale Dynamic Tests", J. Geotech. Geoenv. Eng., DOI:10.1061/(ASCE)GT.1943-5606.0001446, in press, 2016.
- [12] M. Molinari, M. Pozzi, D. Zonta, and L. Battisti. "In-field testing of a steel wind turbine tower", Proc. of the IMAC-XXVIII. February 1-4, Jacksonville, Florida USA, 2010.
- [13] D. Capuani, M. Fantini, and M. Merli. "Un approccio con elementi di contorno per l'interazione dinamica di strutture di fondazione attraverso il suolo", Atti del 9° Conv. Naz. "L'ing. sismica in Italia", 1-10, 1999.